PB82-118308

A Transient Current Monitoring and Electrode Characterization System for a Pulsed Oxygen Electrode

Michigan Univ., Ann Arbor

Prepared for

Environmental Monitoring and Support Lab.
Cincinnati, OH

Oct 81

U.S. Department of Commerce
National Technical Information Service
NTIS.

TECHNICAL REPORT DATA
(Please read Instructions on the reverse before completing)

1. REPORT NO. EPA-600/J-80-342 -	2. Journal Article
3. RE PB82-118308	
4. TITLE AND SUBTITLE A Transient Current Monitoring and Electrode Characterization System For a Pulsed Oxygen Electrode	5. REPORT DATE October 1981
	6. PERFORMING ORGANIZATION CODE 308034
7. AUTHOR(S) K. D. Wise, R. B. Smart, and K. H. Mancy	8. PERFORMING ORGANIZATION REPORT NO.
9. PERFORMING ORGANIZATION NAME AND ADDRESS The University of Michigan Ann Arbor, Michigan 48109	10. PROGRAM ELEMENT NO. C61C1C
	11. CONTRACT/GRANT NO. R 804834
12. SPONSORING AGENCY NAME AND ADDRESS Environmental Monitoring and Support Laboratory U. S. Environmental Protection Agency 26 W. St. Clair Street Cincinnati, Ohio 45268	13. TYPE OF REPORT AND PERIOD COVERED Journal article 12/10/76-12/9/79
	14. SPONSORING AGENCY CODE EPA/600/06
15. SUPPLEMENTARY NOTES	

16. ABSTRACT

Non-steady state voltammetry has been applied to membrane electrodes to provide improved sensitivity as well as independence of stirring. This paper describes a new instrumentation system based on complementary metal oxide-silicon technology for the characterization of a pulsed oxygen electrode. The system provides the necessary timing, analog-to-digital conversion, and digital display of the transient current.

17. KEY WORDS AND DOCUMENT ANALYSIS

a. DESCRIPTORS	b. IDENTIFIERS/OPEN ENDED TERMS	c. COSATI Field/Group

REPRODUCED BY
NATIONAL TECHNICAL
INFORMATION SERVICE
U.S. DEPARTMENT OF COMMERCE
SPRINGFIELD, VA 22161

18. DISTRIBUTION STATEMENT Release to Public	19. SECURITY CLASS (This Report) Unclassified	21. NO. OF PAGES 8
	20. SECURITY CLASS (This page) Unclassified	22. PRICE

EPA Form 2220-1 (Rev. 4-77) PREVIOUS EDITION IS OBSOLETE

EPA-600/J-80-342
Journal Article

Analytica Chimica Acta, 116 (1980) 297—305

A TRANSIENT CURRENT MONITORING AND ELECTRODE CHARACTERIZATION SYSTEM FOR A PULSED OXYGEN ELECTRODE

K. D. WISE

Department of Electrical and Computer Engineering, The University of Michigan, Ann Arbor, Michigan 48109 (U.S.A.)

R. B. SMART[*a] and K. H. MANCY

The Environmental Chemistry Laboratory, School of Public Health, The University of Michigan, Ann Arbor, Michigan 48109 (U.S.A.)

(Received 24th September 1979)

SUMMARY

Non-steady state voltammetry has been applied to membrane electrodes to provide improved sensitivity as well as independence of stirring. This paper describes a new instrumentation system based on complementary metal oxide—silicon technology for the characterization of a pulsed oxygen electrode. The system provides the necessary timing, analog-to-digital conversion, and digital display of the transient current.

Dissolved oxygen voltammetric membrane electrodes have found wide use for in-situ determination of oxygen in natural and waste water, biological fluids, cells, tissues, and non-aqueous media [1—3]. Most of the systems presently available are based on steady-state measurements. The use of a membrane electrode under continuous polarization, however, has the disadvantage of being operated with the lowest possible sensitivity. Under these conditions the sensitivity is dependent on the membrane thickness and permeability, as shown by Mancy et al. [2]. The highest sensitivity should be obtained with very thin membranes, but practical considerations limit the membrane thickness to about 2.54×10^{-3} cm. The cathode area can be increased, but larger electrodes tend to become bulky and generally exhibit excessive residual currents. The use of membranes with higher permeability coefficients can also increase the steady-state response. After several years of laboratory and field experience, the main limitations of steady-state electrode systems have been largely due to: (a) lack of long term sensitivity, (b) low sensitivity, and (c) the need to maintain a certain amount of mixing at the electrode surface.

[*a]Present address: Department of Chemistry, West Virginia University, Morgantown, West Virginia 26506, U.S.A.

The application of a very brief potential pulse to the electrode should make the sensitivity independent of the membrane thickness [2]. The non-steady state voltammetric technique has been reported by Schmid and Mancy [4], Mancy [5], Lilley et al. [6], and Fowler and Oldham [7]. The use of pulsed potential polarization will increase the electrode sensitivity as well as eliminate the need for constant stirring. A problem associated with the pulsed potential technique is the operational need for more sophisticated and cumbersome electronic equipment than that required for steady-state measurements. The current measurement is often done milliseconds after the pulse application, therefore the measurement must be made with a storage oscilloscope or other fast recording device. The application of the pulse is accompanied by an instantaneous rise of current followed by a decay to the steady-state value. The means for providing accurately timed voltage pulses must also be provided. The instrumentation system described below was developed to provide an accurate technique for electrode characterization by using the pulsed potential method; it also provides higher sensitivity in a portable system for field measurements.

EXPERIMENTAL

Apparatus

A YSI (Yellow Springs Instrument Co., Yellow Springs, Ohio) Model 4004 Oxygen Electrode filled with 3.5 M KCl saturated with AgCl was used throughout. The membrane was 1-mil FEP teflon. The area of the platinum cathode was experimentally determined as 9.2×10^{-2} cm^2 [8]. A Tektronix Type 564 storage oscilloscope (Tektronix, Inc., Beaverton, Oregon) was used to record the transient currents. The electrode was calibrated by using the standard Winkler method [9].

Instrumentation

The design of the transient current monitoring system was based on the need for independent control over the pulse amplitude, duration, and frequency (interpulse interval). Complementary metal oxide–silicon (CMOS) technology was selected for this application because it provides low power dissipation, relatively high speed, and a high insensitivity to variations in power supply voltage and ambient temperature. The system consists of several sections, as shown in Fig. 1. The voltage to be applied to the electrode is selected by a potentiometer and is continuously variable between zero and ±1.2 V. This electrode voltage is buffered and applied to the working electrode through a series electronic switch. For three-electrode systems, the reference electrode potential is added to the selected electrode voltage to eliminate the effects of polarization at the anode. An FET-input operational amplifier is used as a non-inverting buffer, to ensure a reference electrode current of less than 20 pA. A second FET-input amplifier senses the current passed by the working electrode and converts it to a voltage with an output

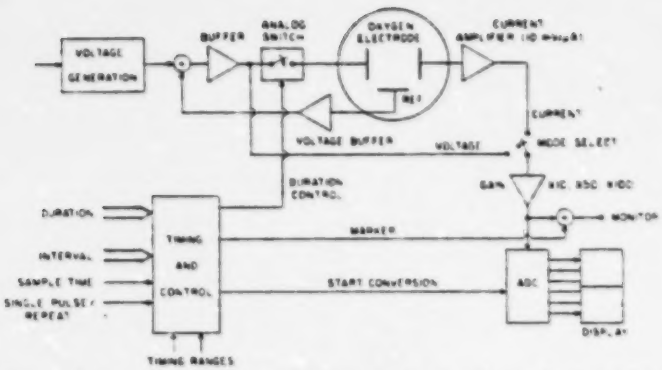

Fig. 1. Schematic of transient current monitoring electrode characterization system.

of 10 mV μA^{-1}. Subsequent amplifiers allow the user to select overall amplifications of 0.1 V μA^{-1}, 0.5 V μA^{-1}, or 1 V μA^{-1}. The resulting signal is available for display on an oscilloscope via a connector on the back of the chassis. The amplification section has a frequency response from d.c. to about 10 kHz.

The pulse duration and interpulse interval are determined by the timing and control section. These parameters are selected by sixteen toggle switches on the front panel, eight of which are used for each parameter. These switches are binarily weighted and are used to preset eight-bit binary counters which are driven by a crystal-generated clock signal. The clock can be adjusted at 1 ms or 10 ms for pulse duration and at 10 ms or 100 ms for pulse interval. The resulting parameter ranges are selectable from 1 ms to 2.55 s for duration and 10 ms to 25.5 s for interval. The pulses may be applied repetitively or individually (single pulse) via front panel switches. These timing intervals are accurate to within 0.3% or better and are stable to within ±20 ppm over the ambient temperature range from 10°C to 40°C.

The sample time on the present system is continuously variable between 5 ms and about 1.5 s in two overlapping ranges which are automatically switched with pulse duration. The sample time is the time at which electrode current is measured. It can be accurately set by using the pulse duration switches to establish first the end of the pulse at the desired sample point, adjusting the variable sample time control to the pulse edge, and then subsequently setting the desired duration. An alternative being considered for future versions of this system is to enter all three timing intervals digitally via a single set of panel switches, storing the desired settings in internal latches, and allowing sample time to be established more easily and with greater stability. A marking pulse is introduced into the electrode current waveform available for display to identify the sample point. Figure 2 shows the current waveforms as well as the marking pulse produced by this system operating with an oxygen electrode.

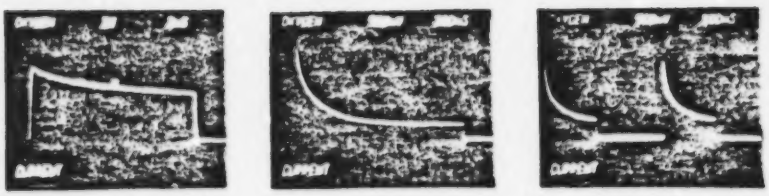

Fig. 2. Typical current waveforms (V vs. time) for an oxygen electrode. $E = -0.8$ V vs. Ag/AgCl; marking pulse defines time of current sampling; (a) pulse duration = 15 ms; (b) pulse duration = 1.55 s; (c) pulse duration = 250 ms. Pulse interval = 300 ms.

In order to quantify the electrode current at the desired sample time, the amplified current waveform is presented to an eight-bit CMOS successive-approximation analog-to-digital converter (ADC). A start signal is generated by the timing section to initiate the conversion at the desired sample time. The conversion time is about 75 μs for eight-bits as used, although the converter (an Analog/Devices AD7570JD) could perform the conversion in as little as 20 μs if required. The output of the converter is an eight-bit binary representation of the current amplitude at the sample time and this information is displayed on two hexadecimal LED displays. Decimal displays could also be used with additional decoding logic.

The eight-bit converter quantizes a 10-V reference voltage into 256 equal intervals, allowing electrode current to be determined with an accuracy of 20 nA or better. For the present electrodes, this corresponds to an error of 20 μg l^{-1} or less in the measured oxygen concentration. Clock noise, thermal noise, and system stability appear consistent with the use of a 10-bit converter, which would increase the accuracy and resolution of the system by an additional factor of four while maintaining the same dynamic range. A panel switch allows the present converter to display the electrode voltage as an alternative to electrode current so that the required level can be accurately adjusted in the field.

This monitoring system has been realized by using commercial integrated circuits on a standard 30-in^2 wire-wrap board. Power dissipation, excluding the displays (which dissipate approximately 1.2 W at 6 V), is less than 0.5 W. The system requires +6 and ±12 V supplies. Both a.c.- and d.c.-powered versions have been realized, the latter operating from rechargeable Gel-cell batteries. Table 1 summarizes the operating characteristics of the system. The small size of the system makes it easily portable for field measurements.

MODEL FOR A PULSED OXYGEN ELECTRODE

The theory of two-layer diffusion current for a membrane electrode has been described in detail by Mancy et al. [2]. The steady-state current is given by:

$$i_{ss} = nFA\,P_m\,C/b \quad (1)$$

where i_{ss} is the steady-state current (A); n is the number of electron equivalents per mole of oxygen; F is the Faraday constant; A is the electrode area (cm^2); P_m is the membrane permeability coefficient ($cm^2\ s^{-1}$); b is the membrane thickness (cm); and C is the bulk oxygen concentration (mol cm^{-3}). Upon application of a very short potential pulse, the current may be described by:

$$i_t = nFA\,(P_m/\pi t)^{1/2}\,C \quad (2)$$

where i_t is the current (A) at time t (s). Equation (2) will be valid only if sufficient time is provided between pulses to re-equilibrate the membrane and electrolyte.

Morris and Faulkner [10] have investigated normal pulse voltammetry, using an open circuit interval and a platinum disc electrode. Equilibration of the diffusion layer during the pulse interval was inhibited by coulostatic discharge of the double layer. At time $t = 0$, a potential step was made to E (see Fig. 4) where subsequent electrolysis is diffusion-limited. This potential was applied for a specific duration and the electrode was then open-circuited. Electrolysis proceeded coulostatically until the potential fell to $E_{1/2}$. The time it took for E to fall back to $E_{1/2}$ was designated as the effective pulse width. At that time the surface flux and hence the electrolysis rate may be regarded as zero. The effective pulse width was described as follows:

$$(t_p)_{eff}^{1/2} = [\pi^{1/2}\,C_d\,(E_{1/2} - E)/2\,nFD^{1/2}\,C^*] + t_p^{1/2} \quad (3)$$

where t_p is the pulse duration (s); $(t_p)_{eff}$ is the effective pulse width (s); C_d is the differential double layer capacitance (farads); $E_{1/2}$ is the half-wave potential (V); E is the applied potential (V); D is the diffusion coefficient ($cm^2\ s^{-1}$); F is the Faraday constant; C^* is the bulk concentration of the reactant (mol cm^{-3}); and n is the number of electrons. The dependence of $(t_p)_{eff}$ on the solution concentration is evident from eqn. (3). Table 2 gives the calculated values for $(t_p)_{eff}$ for a typical oxygen electrode at various t_p and oxygen concentrations.

The thickness of the diffusion gradient, x, caused by oxygen reduction at the electrode surface can be calculated [11] for any pulse duration by

$$C(x,t) = C\{2/\pi^{1/2} \int_0^{x(2Dt)^{-1/2}} e^{-y^2}\,dy\} \quad (4)$$

Examining the point where the bulk oxygen concentration is only 1% different than the concentration at the electrode surface, eqn. (4) can be solved to give $x\,(2\,Dt)^{-1/2} = 1.8$. At $t = 1$ ms and $D_f = 2.4 \times 10^{-5}\ cm^2\ s^{-1}$, the diffusion gradient thickness is calculated as 5.6 μm. This is the approximate thickness of the electrolyte layer for the test electrode. At times greater than 1 ms, it is therefore necessary to consider diffusion in the membrane and the membrane diffusion coefficient, D_m, must be used to solve eqn. (4).

TABLE 1

Characteristics of the transient current monitoring system

Electrode voltage	Continuously adjustable 0 to ±1.2 V; two- or three-electrode operation
Operating modes	Single-pulse or repetitive pulse train
Pulse duration	1 ms to 2.55 s in two overlapping ranges
Pulse interval	10 ms to 25.5 s in two overlapping ranges
Timing accuracy	Less than 0.3% error; temperature drift less than 20 ppm
Current amplification	Selectable: 0.1 V μA^{-1}; 0.5 V μA^{-1}; 1 V μA^{-1}
Sample time	Continuously adjustable, 5 ms to 1.5 s in two overlapping ranges
Display modes	Electrode voltage (±2 mV in high gain position); electrode current (±20 nA in high gain position)
Power dissipation	20 mA at ±12 V; 200 mA at +6 V: 1.7 W total, including displays
Size	240 $in.^3$ (3 × 8 × 10 in.)

The theoretical current given by eqn. (2) is based on the absence of capacitance current; however, the contribution of capacitance current to the total observed experimental current in pulsed electrode voltammetry is well known [12]. The pulse capacitance current is given by

$$i_c = (\Delta E/R) \exp(-t/RC) \quad (5)$$

where i_c is the capacitance current (A); E is the potential change (V); R is the electrode-solution resistance (ohms); C is the electrode capacitance (farads); and t is the pulse duration (s).

RESULTS AND DISCUSSION

The instrumentation system was originally designed to hold the electrode at 0 V during the pulse interval and step to −0.8 V for the pulse duration. Under these conditions, very little current difference was observed for large differences in oxygen concentration. In addition to the expected cathodic faradaic current observed during the pulse duration, an anodic discharge current was also observed upon pulse termination. This condition is illustrated in Fig. 3. The anodic current arises in part from the discharge of the electrical double layer when the electrode is forced back to 0 V. Also, when operating in the pulse mode, sufficient time must be given between pulses for the electrode to become depolarized. If this does not happen, a thick diffusion layer similar to that resulting from steady-state operation will build up, reducing electrode response.

In the light of these results, the instrument was modified to allow the electrode to float at open-circuit potential during the pulse interval as shown in Fig. 4. The open-circuit interval condition prevented the electrode double layer from completely discharging and thus reducing the charging current on the subsequent pulse. This modification greatly improved the system per-

TABLE 2

Calculated effective pulse widths for various oxygen concentrations and pulse durations

$[O_2]$ (mg l^{-1})	$(t_p)_{eff}$ (ms)			$[O_2]$ (mg l^{-1})	$(t_p)_{eff}$ (ms)		
	t_p = 50 ms	t_p = 100 ms	t_p = 500 ms		t_p = 50 ms	t_p = 100 ms	t_p = 500 ms
8	64	119	542	4	80	140	585
7	66	122	548	3	91	154	615
6	69	125	555	2	116	187	677
5	73	132	569	1	208	300	882

formance, allowing the electrode characteristics to be examined. The open-circuit potential, while variable, was found to be considerably more negative than 0 V.

Current versus oxygen concentration for various pulse durations and an interval of 2 s was recorded using the instrument described, and these data are given as the open points in Fig. 5. The sample time was just prior to pulse termination in all cases. Theoretically, the relationship between current and concentration should have been linear according to eqn. (2), but breaks were observed at 100-ms and 150-ms pulse durations. A series of similar experiments was done with the potential and timing controlled by the instrument

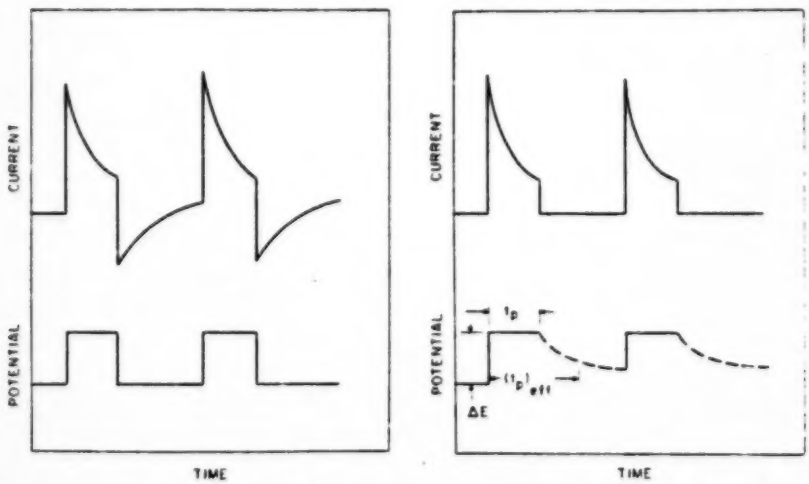

Fig. 3. Current–potential waveform for pulse potential voltammetry with closed-circuit interval.

Fig. 4. Current–potential waveform for pulse potential voltammetry with open-circuit interval. ΔE, applied potential; t_p, pulse duration; $(t_p)_{eff}$, effective pulse duration.

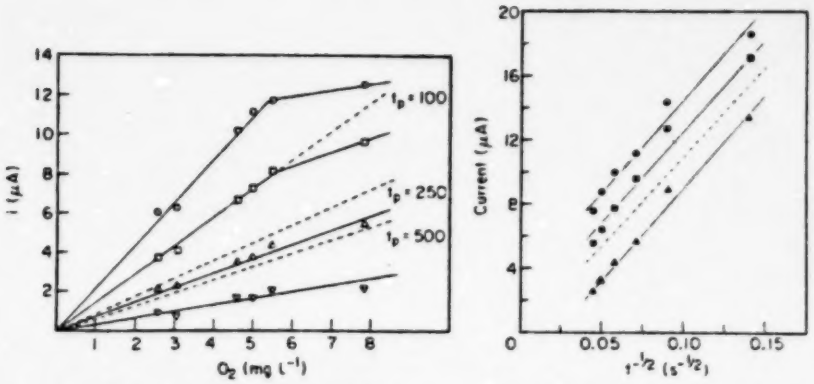

Fig. 5. Calibration curves for the pulsed oxygen electrode. Dashed lines are theoretical for indicated t_p; (○) 100 ms; (□) 150 ms; (△) 250 ms; (▽) 500 ms pulse duration; pulse interval, 5 s.

Fig. 6. Electrode response at various pulse durations and intervals. Dashed line is theoretical current.

but with current levels determined by photographing the current at a 500-ms pulse duration and then reading the reduction currents at shorter pulse durations from the photograph. The data exhibited the expected linear relationship at all pulse durations and the effect of pulse duration on electrode sensitivity, ϕ, is evident from Table 3. The sensitivity for the 50-ms pulse is six times higher than steady state.

The breaks shown in Fig. 5 can be explained by examination of the effective pulse widths and oxygen concentrations at these times. With a t_p of 100 ms and an oxygen concentration of 8 mg l^{-1}, the $(t_p)_{eff}$ obtained from Table 2 is 119 ms. In this case the currents observed by both methods should be similar; however, as Fig. 5 shows, the currents differ experimentally by several μA. By means of eqn. (5), the charging current at 100 ms is calculated to be 6.1 μA (C = 25 F cm^{-2}, R = 30 K, E = −0.8 V). This might explain the difference in the two sets of data at this time and concentration. At lower oxygen concentrations the effect of $(t_p)_{eff}$ is much greater (Table 2) and the observed current must be less than expected. Apparently, a point is gradually reached where the oxygen concentration is no longer sufficient to remove E to $E_{1/2}$ before the subsequent pulse. With a t_p of 500 ms and an oxygen concentration of 8 mg l^{-1}, $(t_p)_{eff}$ is 542 ms and the two sets of data

TABLE 3

Effect of pulse duration on the pulsed voltammetric membrane oxygen electrode for a pulse interval of 2 s

Pulse duration (ms)	50	100	150	250	500	ss
ϕ(μA mg^{-1} l)	1.51	1.09	0.81	0.66	0.34	0.25

should again be similar; in this case, they are, because the charging current is negligible. At the same t_p but with an oxygen concentration of only 1 mg l^{-1}, $(t_p)_{eff}$ is about 1.5 t_p; however, the difference in current at this pulse time is also negligible.

Data obtained by applying a 500-ms pulse duration and sampling the current at shorter times were taken for different oxygen concentrations at pulse intervals of 3 and 5 s. The theoretical current for an oxygen concentration of 8 mg l^{-1} at different pulse durations was calculated from eqn. (2) and is plotted as the dashed line in Fig. 6 versus the reciprocal square root of the pulse duration. The experimental currents were also plotted for the different time intervals. The agreement between the slopes is excellent. Experimental currents were higher than predicted by eqn. (2) possibly because of an error in the selection of a permeability coefficient (known to change from batch to batch) and/or the electrode area determination.

Conclusions

The transient current monitoring instrumentation system has been shown to be a very useful device for pulsed electrode characterization. It has eliminated the need for using an oscilloscope to record transient current, making it portable and suitable for field measurements. In order to achieve still greater flexibility in investigating transient electrode phenomena, an all-CMOS microcomputer-controlled instrumentation system has also been developed. This system should allow correction for the effects of secondary parameters, such as temperature, which can also influence electrode response and will be reported in a separate paper.

The authors gratefully acknowledge the many contributions of K. Holloway, N. Ho, and J. C. Huang in the construction and testing of the instrumentation system. This work was supported by U.S. Environmental Protection Agency Grant No. R804834-01-1.

REFERENCES

1 K. H. Mancy and T. Jaffe, Analysis of Dissolved Oxygen in Natural and Waste Waters, U.S. Dept. HEW, Public Health Service, Publ. No. 999-WP-37, April 1966.
2 K. H. Mancy, D. A. Okun, and C. N. Reilly, J. Electroanal. Chem., 4 (1962) 65.
3 I. Fatt, Polarographic Oxygen Sensors, CRC Press, Cleveland, OH, 1976.
4 M. Schmid and K. H. Mancy, Schweitzerische für Hydrologie, 32 (1970) 328.
5 K. H. Mancy, in W. A. Adams (Ed.), Chemistry and Physics of Aqueous Gas Solutions, The Electrochemical Society, Princeton, NJ, 1976.
6 M. Lilley, J. Story, and R. Raible, J. Electroanal. Chem., 23 (1969) 425.
7 J. K. Fowler and K. B. Oldham, in W. A. Adams (Ed.), Chemistry and Physics of Aqueous Gas Solutions, The Electrochemical Society, Princeton, NJ, 1976.
8 R. Adams, Electrochemistry at Solid Electrodes, M. Dekker, New York, 1969.
9 Standard Method for the Examination of Water and Wastewater, 14th edn., Am. Public Health Assoc., 1976.
10 J. L. Morris and L. R. Faulkner, Anal. Chem., 49 (1977) 489.
11 J. Crank, The Mathematics of Diffusion, Clarendon Press, Oxford, 1956.
12 P. Delahay, New Instrumental Methods in Electrochemistry, Interscience, New York, 1954.